Herb Hydraulics: Inter- and Intraspecific Variation in Three *Ranunculus* Species[1][OPEN]

Markus Nolf[2]*, Andrea Rosani, Andrea Ganthaler, Barbara Beikircher, and Stefan Mayr

Institute of Botany, University of Innsbruck, 6020 Innsbruck, Austria

ORCID IDs: 0000-0001-5374-3113 (M.N.); 0000-0001-7374-2353 (A.R.); 0000-0002-3319-4396 (S.M.).

The requirements of the water transport system of small herbaceous species differ considerably from those of woody species. Despite their ecological importance for many biomes, knowledge regarding herb hydraulics remains very limited. We compared key hydraulic features (vulnerability to drought-induced hydraulic decline, pressure-volume relations, onset of cellular damage, in situ variation of water potential, and stomatal conductance) of three *Ranunculus* species differing in their soil humidity preferences and ecological amplitude. All species were very vulnerable to water stress (50% reduction in whole-leaf hydraulic conductance [k_{leaf}] at −0.2 to −0.8 MPa). In species with narrow ecological amplitude, the drought-exposed *Ranunculus bulbosus* was less vulnerable to desiccation (analyzed via loss of k_{leaf} and turgor loss point) than the humid-habitat *Ranunculus lanuginosus*. Accordingly, water stress-exposed plants from the broad-amplitude *Ranunculus acris* revealed tendencies toward lower vulnerability to water stress (e.g. osmotic potential at full turgor, cell damage, and stomatal closure) than conspecific plants from the humid site. We show that small herbs can adjust to their habitat conditions on interspecific and intraspecific levels in various hydraulic parameters. The coordination of hydraulic thresholds (50% and 88% loss of k_{leaf}, turgor loss point, and minimum in situ water potential) enabled the study species to avoid hydraulic failure and damage to living cells. Reversible recovery of hydraulic conductance, desiccation-tolerant seeds, or rhizomes may allow them to prioritize toward a more efficient but vulnerable water transport system while avoiding the severe effects that water stress poses on woody species.

The resistance of terrestrial plant species to water stress is an important determinant of their spatial distribution (Engelbrecht et al., 2007), and in a globally changing climate, resistance to water stress-induced damage to the water transport system is an essential parameter for the prediction of species survival and future changes in biodiversity and species composition. The hydraulic vulnerability to drought-induced embolism in woody species is adjusted to their environmental conditions on a global scale (Choat et al., 2012), but increased hydraulic safety entails several tradeoffs, such as transport efficiency, as plants can reduce the risk of hydraulic failure by the formation of smaller and hydraulically less efficient conduits (Tyree et al., 1994; Wagner et al., 1998, Gleason et al., 2016).

While many studies have dealt with the hydraulics of woody species (Maherali et al., 2004; Choat et al., 2012), the hydraulic characteristics of small herbaceous species are largely understudied, and our knowledge regarding their water transport system, including vulnerability to drought-induced loss of conductivity, remains very limited (Kocacinar and Sage, 2003; Brodribb and Holbrook, 2004; Iovi et al., 2009; Holloway-Phillips and Brodribb, 2011a; Tixier et al., 2013). Yet, herbs play an important ecological role in many biomes, such as grasslands and the alpine zone (Billings and Mooney, 1968; Gilliam, 2007; Scholz et al., 2010), and represent a significant percentage of crop plants (Monfreda et al., 2008); therefore, they are interesting from an ecophysiological viewpoint.

The requirements of the water transport system of herbs differ in several ways from those of woody species (Mencuccini, 2003). First, transport distances and supported leaf areas are much smaller in herbs, and reversible extraxylary limitations (Brodribb and Holbrook, 2005; Kim and Steudle, 2007) may have a stronger effect on hydraulic conductivity. Second, herbs often do not feature an essential, lignified main axis designed for long-term functioning, in which hydraulic failure may mean whole-plant mortality. Third, small plants may more easily restore water transport capacity in the case of embolism formation, because, due to smaller size, a water potential (Ψ) at or near zero can be reached quickly under favorable conditions due to positive root pressure (Tyree and Sperry, 1989; Tyree and Ewers, 1991; Stiller and Sperry, 2002; Tyree and Zimmermann, 2002; Ganthaler and Mayr, 2015).

[1] This work was supported by the Austrian Science Fund (FWF project nos. I826–B25 and T–667) and the Austrian Academy of Sciences (DOC fellowship to M.N.).

[2] Present address: Hawkesbury Institute for the Environment, Western Sydney University, Richmond, New South Wales 2753, Australia.

* Address correspondence to m.nolf@westernsydney.edu.au.

The author responsible for distribution of materials integral to the findings presented in this article in accordance with the policy described in the Instructions for Authors (www.plantphysiol.org) is: Markus Nolf (m.nolf@westernsydney.edu.au).

The study was led by M.N. and S.M.; all authors contributed to the experimental design and methodical developments; A.G., A.R., B.B., and M.N. conducted field and laboratory measurements and performed data analysis; M.N. prepared the article with contributions of all the authors; S.M. supervised and complemented the writing.

[OPEN] Articles can be viewed without a subscription.

www.plantphysiol.org/cgi/doi/10.1104/pp.15.01664

Thus, herbs may not be as threatened by drought-induced failure as taller woody species.

Hydraulic failure occurs when vulnerability thresholds are exceeded under water stress and the xylem tension is suddenly released as water is replaced by air, effectively blocking water transport in the affected conduits (Tyree and Zimmermann, 2002). Vulnerability to drought-induced embolism can thus be analyzed hydraulically by measuring decreases in conductance during increasing water stress (Sperry et al., 1988a; Cochard, 2002; Cochard et al., 2013), by noninvasive imaging of xylem water content (Choat et al., 2010; Brodersen et al., 2013; Cochard et al., 2015), or indirectly by monitoring of ultrasonic acoustic emissions (UE) which occur during the spontaneous energy release at embolism formation (Milburn and Johnson, 1966; Mayr and Rosner, 2011; Ponomarenko et al., 2014). However, the usability of UE analysis to noninvasively study hydraulic vulnerability remains under discussion (Sandford and Grace, 1985; Kikuta, 2003; Wolkerstorfer et al., 2012; Cochard et al., 2013; Rosner, 2015).

On the leaf level, desiccation may induce turgor loss, decreases in mesophyll conductance (Kim and Steudle, 2007; Scoffoni et al., 2014), or cell collapse (Blackman et al., 2010; Holloway-Phillips and Brodribb, 2011a), and limit hydraulic conductance, gas exchange, and thus photosynthesis before embolism occurs. When water stress increases further, living cells may incur damage resulting in tissue and leaf mortality.

In this study, we compared key hydraulic features (vulnerability to drought-induced loss of conductance as measured via hydraulic flow and xylem staining, pressure-volume relations, and the onset of cellular damage) of three species from the genus *Ranunculus*, which is distributed almost worldwide and contains species adapted to dry and humid habitats as well as species with broad ecological amplitude. We hypothesized that herbaceous species would be more vulnerable to water stress than woody species but also would show interspecific and intraspecific adjustments in hydraulic vulnerability based on the water availability of their respective habitats. Namely, the hydraulics of species with narrow ecological amplitude were hypothesized to reflect their respective habitat conditions, and broad-amplitude species should show adequate intraspecific variation to enable growth in dry and humid habitats.

RESULTS

Volumetric soil water content (SWC) at field capacity was 40.4% (dry site), 51% (humid site; *Ranunculus acris*), and 30.4% (humid site; *Ranunculus lanuginosus*). Relative SWC after 7 d of rain-free weather was above 90% at the humid sites and 43% to 58% at the dry site (Table I). The low field capacity SWC of the second humid site was due to the soil composition (thin layer of humus and litter on top of gravel substrate), yet the SWC remained constant due to the humid conditions inside the gorge. The reason for a relative soil water content (SWCrel) of 100% or greater at this site may lie in water seeping through the slope from uphill soils. Ecological indicator values for the study species and cooccurring species at the sampling sites supported the observed differences in water availability: averaged humidity values were 4.4 at the dry site and notably higher at 5.5 (*R. acris*) and 5.7 (*R. lanuginosus*) at the humid sites (Table I). At the dry site, *Ranunculus bulbosus* (humidity index of 3; indicator for dry sites) and *R. acris* (humidity index of 6; indicator for humid sites but broad amplitude) were accompanied by dry-habitat species such as *Bromus erectus*, *Knautia arvensis*, and *Lotus corniculatus*. In contrast, at the humid sites, *R. lanuginosus* (humidity index of 6) and *R. acris* were cooccurring with other species typical for moist habitats, including *Polygonum bistorta*, *Rumex conglomeratus*, *Urtica dioica*, and *Solanum dulcamara* (Supplemental Table S1).

The turgor loss point (TLP) was least negative in *R. lanuginosus* at a leaf water potential (Ψ_{leaf}) of -1.1 ± 0.1 MPa and was reached at -1.4 ± 0.0 MPa in *R. bulbosus* and at -1.6 ± 0.1 to -1.7 ± 0.1 MPa in *R. acris* (Table I). The osmotic potential (Π_0) followed a similar trend at -0.9 ± 0.1 MPa (*R. lanuginosus*), -1.3 ± 0.0 MPa (*R. bulbosus*), and -1.4 ± 0.1 to -1.5 ± 0.1 MPa (*R. acris*). In contrast, the modulus of elasticity was lowest (i.e. cells were more elastic) at 9.6 ± 1.9 MPa in *R. lanuginosus* and 1.5 to 2.5 times higher in the other species (*R. bulbosus*, 16.7 ± 1.3 MPa; and *R. acris*, 20.4 ± 4.4 to 24.9 ± 3.6 MPa).

Maximum whole-leaf hydraulic conductance ($k_{leaf\,max}$) was between 23.4 and 28 mmol m^{-2} s^{-1} MPa^{-1} and did not differ between species (Table I). Hydraulically measured water potential at 50% loss of leaf hydraulic conductance (P_{k50}) was least negative in *R. lanuginosus* (-0.2 MPa) and more negative in *R. acris* and *R. bulbosus* (-0.6 to -0.8 MPa; Table II; Fig. 1). Similarly, water potential at 88% loss of leaf hydraulic conductance (P_{k88}) was highest in *R. lanuginosus* (-0.4 MPa) and significantly more negative in the other two species (-1.5 to -3.3 MPa; Table II; Fig. 1).

Conductive xylem staining in *R. acris* (dry) showed the first notable signs of embolism in minor leaf veins and vascular bundles at -2 MPa, with significant losses of even first-order leaf veins by -2.7 MPa (Fig. 2).

Significant cellular lysis started at more negative Ψ than P_{k50}, with water potential at 12% of cellular lysis (P_{12CL}) between -1.1 and -2 MPa (Table II; Fig. 3), whereas thresholds for cell damage did not correspond to humidity conditions. In contrast, the onset of UE was observed at less negative Ψ than hydraulic vulnerability thresholds, with peak activity at -1.1 MPa or greater (Supplemental Table S2; Supplemental Fig. S1).

In situ, species reached minimum leaf water potential (Ψ_{min}) of -0.4 ± 0.1 to -2.2 ± 0.1 MPa, whereby Ψ_{min} was lower at the dry site (Table I; Fig. 4). In contrast, stomatal conductance (g_s) exhibited considerable variability at more negative Ψ. Maximum stomatal conductance ($g_{s\,max}$) was between 492.1 ± 86.1 and 885 ± 37.3 mmol m^{-2} s^{-1} and did not reflect soil humidity differences between sites (Table I; Fig. 4). The

Table I. *SWC_{rel} (measured in summer 2014 and 2015; n = 10), averaged humidity value (n = 10–13), $k_{leaf\,max}$ (n = 5), TLP (n = 5), diurnal Ψ_{min} (n = 3 [Fig. 4; Supplemental Fig. S2]), and diurnal $g_{s\,max}$ (n = 5 [Fig. 4; Supplemental Fig. S2])*

Values are means ± SE. Letters indicate significant differences in each row ($P < 0.05$).

Species	SWC_{rel} (2014)	SWC_{rel} (2015)	Humidity Value	TLP	$k_{leaf\,max}$	Ψ_{min}	$g_{s\,max}$
	%	%		MPa	mmol m^{-2} s^{-1} MPa^{-1}	MPa	mmol m^{-2} s^{-1}
R. bulbosus (dry)	57.57 ± 4.03 a	43.29 ± 2.42 a	4.40 ± 0.34 a	−1.43 ± 0.02 a	28.00 ± 0.78 a	−1.70 ± 0.03 a	537.7 ± 105.3 a
R. lanuginosus (humid)	102.72 ± 6.14 b	98.34 ± 2.31 b	5.69 ± 0.26 b	−1.14 ± 0.05 b	27.77 ± 1.12 a	−0.42 ± 0.12 b	492.1 ± 86.1 a
R. acris (dry)	57.57 ± 4.03 a	43.29 ± 2.42 a	4.40 ± 0.34 a	−1.72 ± 0.08 c	23.40 ± 0.42 a	−2.20 ± 0.06 c	756.6 ± 195.9 a
R. acris (humid)	93.40 ± 1.87 b	90.59 ± 1.30 c	5.50 ± 0.23 b	−1.63 ± 0.05 a,c	24.06 ± 0.78 a	−1.48 ± 0.15 a	885.0 ± 37.3 a

progression of Ψ_{leaf} and g_s in the field (illustrated in Fig. 4 for *R. acris*) revealed that g_s was reduced in all species when Ψ_{min} was reached. Theoretical whole-leaf hydraulic conductance (k_{leaf}) as calculated from measured Ψ_{leaf} and transpiration (E; based on measured g_s and climate data from the closest weather station at approximately 3 km distance) agreed well with k_{leaf} predicted from vulnerability curves. However, vapor pressure deficit and transpirational demand were expected to be lower in the lowest canopy layer than calculated here (Wohlfahrt et al., 2010). Both Ψ_{leaf} and g_s were compared on representative, sunny days, but environmental conditions (wind or prolonged drought stress) may lead to more extreme values. Because of windy (*R. bulbosus*) or shady (*R. lanuginosus*; due to its understory gorge habitat) conditions during in situ measurements (Supplemental Fig. S2), diurnal variation data for only *R. acris* were used for further interpretation.

DISCUSSION

We found that all studied species were generally vulnerable to dehydration, but differences between species/populations reflected the humidity conditions of their respective habitats.

Sites differed in their water availability, as the SWC_{rel} between dry and humid sites differed significantly after only 7 d without precipitation. At the dry site, SWC_{rel} decreased to less than 60% of field capacity after only 1 week of rain-free weather, whereas the humid sites experienced hardly any reduction in soil humidity. The low SWC at the humid site of *R. lanuginosus*, which was due to soil composition, was compensated by the humid conditions inside the gorge, so that SWC_{rel} did not decrease during the rain-free period. Species composition and ecological indicator values supported the distinction between dry and humid sites (Table I; Supplemental Table S1).

Herb Hydraulics

k_{leaf} is known to vary widely across species and plant functional types, with an average k_{leaf} of 11.5 ± 0.9 mmol m^{-2} s^{-1} MPa^{-1} across 107 woody and herbaceous species and with individual species ranging between 0.8 and 49 mmol m^{-2} s^{-1} MPa^{-1} (Sack and Holbrook, 2006). Leaf hydraulic efficiency in herbaceous crops was above average at 24.1 ± 2.2 mmol m^{-2} s^{-1} MPa^{-1} (Sack and Holbrook, 2006), and other, noncultivated herbaceous angiosperms in the literature had values between 2.7 and 22 mmol m^{-2} s^{-1} MPa^{-1} (Brodribb and Holbrook, 2004; Bunce, 2006; Galmes et al., 2007). Our study species were within the range known for herbaceous plants and, therefore, showed much higher hydraulic efficiency than woody species (Table I; Fig. 1).

Leaf hydraulic vulnerability studies on small herbaceous species found 50% reduction in k_{leaf} between −1 and −1.8 MPa in perennial grasses (Brodribb and Holbrook, 2004; Holloway-Phillips and Brodribb, 2011a, 2011b). Woody species generally feature leaves that are less vulnerable to water stress, with an

Table II. *Water potential at 50 and 88% loss of leaf hydraulic conductance (P_{k50} and P_{k88}; MPa), and 12% of cellular lysis (P_{12CL}; MPa).*

Thresholds were computed after fitting the reparameterized Weibull function (Ogle et al., 2009) to vulnerability curves. Values are means (MPa) and 95% confidence intervals. Letters indicate significant differences in each row ($P < 0.05$).

Species	Leaf Hydraulic Vulnerability		Electrolyte Leakage
	P_{k50}	P_{k88}	P_{12CL}
R. bulbosus (dry)	−0.57 (−0.63, −0.48) a	−1.53 (<−1.55, −1.31) a	−1.11 (−1.53, −0.84) a
R. lanuginosus (humid)	−0.15 (−0.19, −0.10) b	−0.44 (−0.60, −0.35) b	−1.16 (−1.47, −0.88) a
R. acris (dry)	−0.82 (−1.08, −0.54) a	−3.27 (<−3.27, −2.64) c	−2.02 (−2.43, −1.64) b
R. acris (humid)	−0.73 (−0.93, −0.50) a	−2.84 (<−3.15, −2.25) c	−2.02 (−2.29, −1.62) b

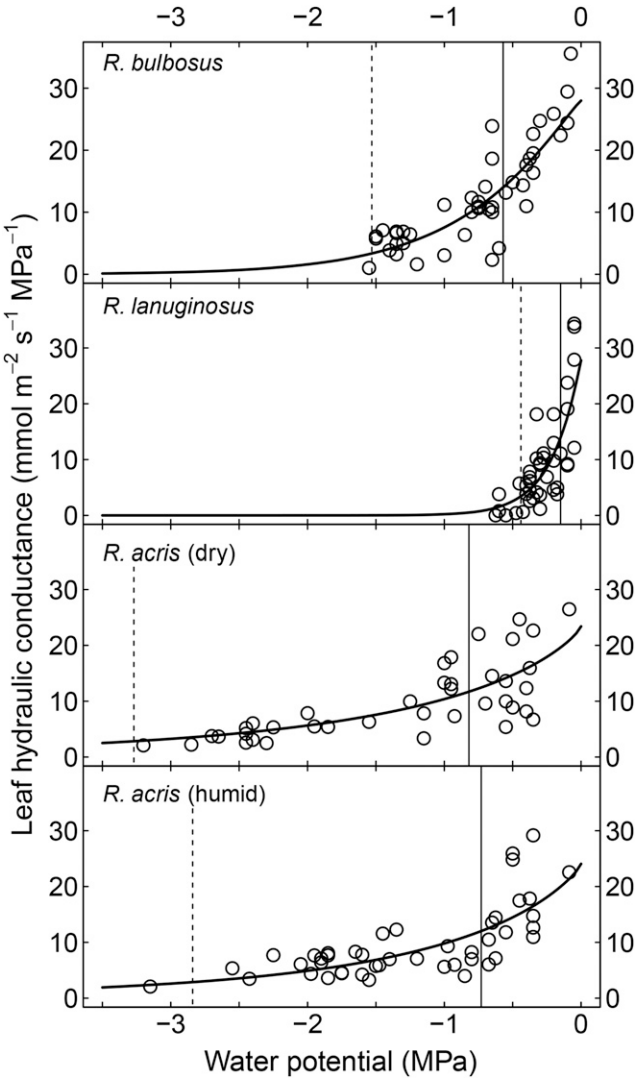

Figure 1. k_{leaf} versus Ψ in *R. bulbosus*, *R. lanuginosus*, and dry and humid *R. acris* populations measured with the non-steady state leaf rehydration technique. Vertical lines indicate fitted hydraulic vulnerability parameters P_{k50} (solid) and P_{k88} (dashed). Curves were extrapolated using the same equation and parameters used for vulnerability curves (Eq. 2).

average P_{k50} of −1.8 ± 0.1 MPa across 81 woody angiosperm species when measured with comparable methods (Nolf et al., 2015). Although some of these species also had very vulnerable leaves at P_{k50} of −1 MPa or greater (Hao et al., 2008; Chen et al., 2009; Blackman et al., 2012; Guyot et al., 2012), the majority of previously studied species exhibited P_{k50} of −1.5 MPa or less and down to −4.3 MPa (Sack and Holbrook, 2006; Blackman et al., 2010; Johnson et al., 2012; Nardini et al., 2012; Bucci et al., 2013). Accordingly, stems were typically also more vulnerable to drought-induced hydraulic failure in herbs (−1 to −3.8 MPa; Kocacinar and Sage, 2003; Rosenthal et al., 2010; Tixier et al., 2013; Nolf et al., 2014) than in woody species (−0.1 to −14.1 MPa, and −3.4 ± 0.1 MPa across 480 species; Choat et al., 2012).

Leaf hydraulic analysis in our study showed that all three *Ranunculus* spp. were very vulnerable to water stress, with P_{k50} of −0.8 MPa or greater in k_{leaf} across all species (Table II; Fig. 1). However, xylem staining indicated that early hydraulic conductivity losses at moderate Ψ were due to extraxylary, likely reversible, effects rather than xylem embolism. Stained petiole sections and leaves revealed loss of conductivity due to embolism and suggested an estimated 50% loss of xylem hydraulic conductivity due to embolism of −2 MPa or less in *R. acris* (dry; Fig. 2). Thus, despite the fact that plants were still very vulnerable to drought, it is important to stress that the leaf hydraulics method employed measured bulk hydraulic conductivity, including both xylary and extraxylary (e.g. mesophyll) pathways, and reflected the total effect on symplastic and apoplastic transport. Interestingly, stained cross sections also indicated an all-or-nothing effect, where, in most cases, individual vascular bundles lost all conductivity at once (Fig. 2C).

Compared with the staining results, ultrasonic activity was observed at much less negative Ψ than expected (Supplemental Table S2; Supplemental Fig. S1). We believe that other signal sources unrelated to water transport (e.g. parenchyma and sclerenchyma) were responsible for a considerable portion of emissions, skewing the acoustic analysis. Thus, interpretation of UE analyses on herbs is difficult and requires further methodical optimization.

With daily Ψ_{min} being 0.3 to 1.4 MPa lower than P_{k50}, at least two of our species would incur significant water transport reduction during the course of the day (Tables I and II; Stiller et al., 2003), limiting transpiration and, thus, according to Ohm's law, preventing a further decrease of Ψ. However, the staining experiment suggests that embolism plays only a minor role in hydraulic decline at the observed in situ Ψ (Fig. 2); therefore, water transport is limited mainly by reversible extraxylary effects (e.g. turgor loss or cell collapse and associated mesophyll conductance losses; Brodribb and Holbrook, 2005; Kim and Steudle, 2007; Blackman et al., 2010; Holloway-Phillips and Brodribb, 2011a; Scoffoni et al., 2014).

Like significant hydraulic transport reductions, the TLP is another critical point plants need to avoid so they can maintain photosynthesis, transport of solutes, and growth (Frensch and Hsiao, 1994; Kramer and Boyer, 1995; Brodribb and Holbrook, 2003; Bartlett et al., 2012). In our study species, the TLP was lower than hydraulic P_{k50}, indicating that all studied species would face notable reductions in transport capacity under limited water supply before leaves would lose turgor (Tables I and II). This indicates that the impairment of whole-leaf water transport is the first critical event during water stress. Pressure-volume analysis revealed that TLPs in this study were determined mainly by the Π_0, whereas a mediating, opposite effect caused by the observed trends in bulk elasticity was small. Only in *R. lanuginosus*, the high elasticity may have compensated for the species' weak water-holding capability (high Π_0) to maintain turgor longer.

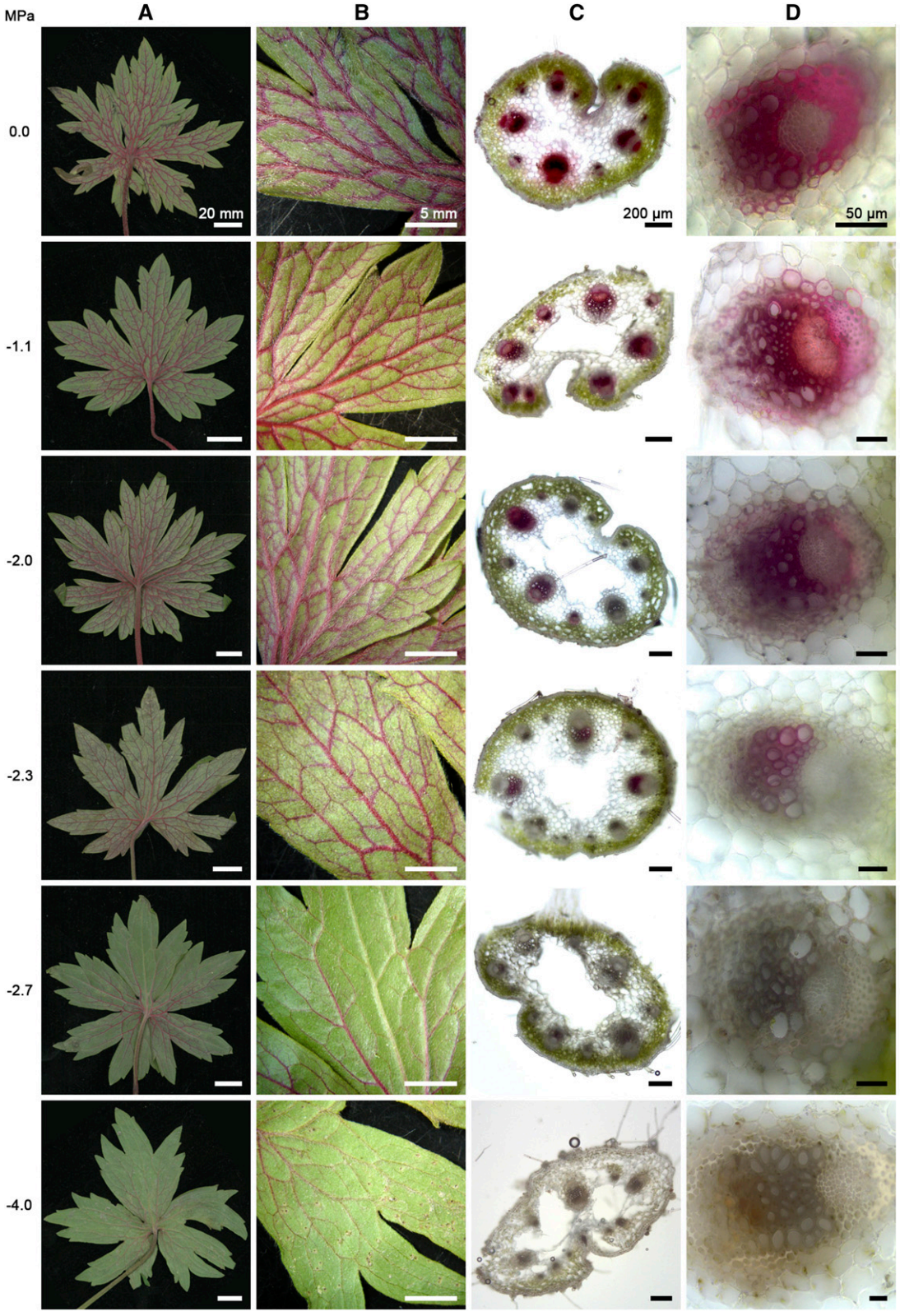

Figure 2. Stained leaf laminas and petiole cross sections of *R. acris* (dry) indicating loss of hydraulic conductance at increasing levels of dehydration. Conducting elements appear red, while embolized conduits remain unstained. A, Leaf lamina undersides and petioles. Bars = 20 mm. B, Leaf lamina details. Bars = 5 mm. C, Petiole cross sections approximately 3 cm from the laminas. Bars = 200 μm. D, Vascular bundle details from cross sections. Bars = 50 μm.

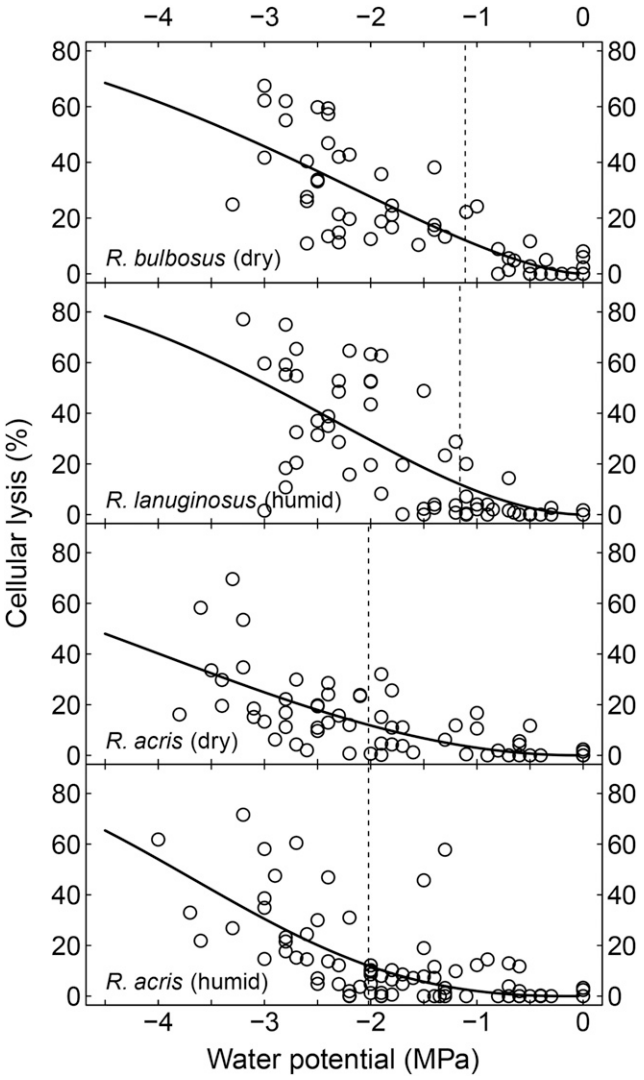

Figure 3. Cellular lysis (percentage of maximum after autoclaving) versus Ψ in *R. bulbosus*, *R. lanuginosus*, and dry and humid *R. acris* populations. Vertical lines (dashed) indicate the onset of damage to living cells (P_{12CL}). Curves were extrapolated using the same equation and parameters used for vulnerability curves (Eq. 2).

Electrolyte leakage analysis showed that desiccation-induced damage to living cells (P_{12CL}) would only begin long after significant hydraulic decline (P_{k50}; Table II; Figs. 1 and 3). Since leaves were benchtop dehydrated for up to several hours, we would expect an even higher apparent vulnerability due to continuous exposure to low Ψ in these measurements, compared with shorter in situ stress peaks followed by stomatal regulation and Ψ recovery. Thus, living cells were well protected from desiccation-induced cell damage, as found previously by other authors (Vilagrosa et al., 2010; Beikircher et al., 2013). Interestingly, plants from dry habitats did not appear more resistant to cell damage than plants from humid sites (Table II; Fig. 3). While we sampled only fully developed, mature leaves, we note that *R. bulbosus* required measurement 1 to 2 months earlier than other species due to their summer dormancy (see "Study Sites and Plant Material").

Interspecific Differences

Study species with narrow ecological amplitude (*R. bulbosus* and *R. lanuginosus*) showed significant differences in some key hydraulic parameters (TLP, P_{k50}, and P_{k88}), which were correlated with their respective soil humidity conditions. The corresponding trend in daily Ψ_{min} further indicated that Ψ_{leaf} was regulated near P_{k88} in both species. In contrast, $k_{leaf\,max}$, daily $g_{s\,max}$, and P_{12CL} revealed no corresponding trend, which suggests that these parameters are more evolutionarily conserved.

The hydraulics of *R. acris*, with its broad ecological amplitude, showed characteristics closer to the drought-adapted species (e.g. P_{k50} and P_{k88}; Table II) regarding hydraulic measurements and did not reveal the intermediate values we expected. The fact that P_{k50}, P_{k88}, and P_{12CL} were more negative in *R. acris* than in *R. bulbosus* may suggest that, although *R. acris* also occurs frequently in humid sites, it is generally well adapted for dry habitats. Another possible explanation is that, by dying back to perennial tubers in early summer, *R. bulbosus* effectively avoids periods of intense water stress in summer and autumn (Coles, 1973; Sarukhan, 1974; Larcher, 1995).

Intraspecific Acclimation

Within-species variation in hydraulic parameters was found previously for woody species (Matzner et al., 2001; Cochard et al., 2007; Beikircher and Mayr,

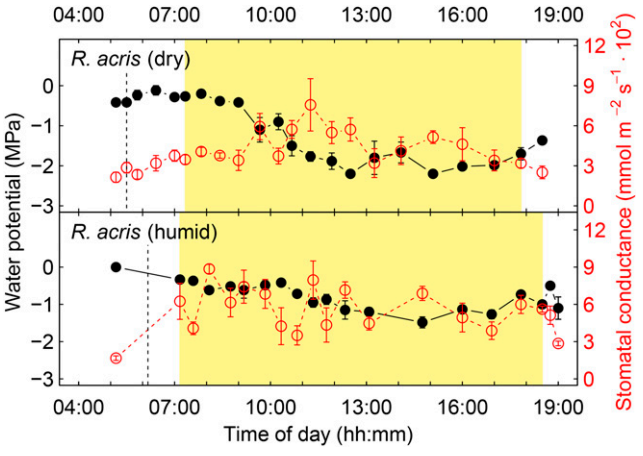

Figure 4. Diurnal variation of Ψ (MPa; black circles, solid black lines) and g_s (mmol m^{-2} s^{-1}; red open circles, dashed red lines) in *R. acris* populations on dry and humid sites. Vertical lines (dashed) indicate meteorological dawn, and yellow areas indicate direct sunlight. Values are means ± SE.

2009; Charra-Vaskou et al., 2012) and herbaceous species (Holste et al., 2006; Tixier et al., 2013; Nolf et al., 2014). *R. acris* was chosen for its wide distribution and broad ecological amplitude and showed trends for intraspecific variation. While most of the species' hydraulic traits indicated adjustment to dry habitats when compared with other species (Tables I and II; Figs. 1, 3, and 4), plants from the dry site tended to have more negative vulnerability thresholds (P_{k50} and P_{k88}), TLP, and daily Ψ_{min} than conspecific plants from the humid site. Thus, we suggest that the intraspecific variability in hydraulic parameters of *R. acris* allows the species to retain fitness over a range of humidity conditions (Rejmanek, 1999) and is a major factor determining its wide distribution, as found for other herbaceous species (Hao et al., 2013; Nolf et al., 2014). Interestingly, the onset of desiccation-induced cellular damage (P_{12CL}; Table II; Fig. 3) was constant across sites, indicating that this parameter was not subject to adjustment.

CONCLUSION

Overall, all of our study species were very vulnerable to water stress, even *R. bulbosus*, which is a typical species of dry meadows. However, the first effect of drought in these species was found to be a loss of k_{leaf} at moderate Ψ based on extraxylary pathways rather than embolism formation. This may be an effective, easily reversible way for plants to avoid critical decreases in Ψ and subsequent hydraulic failure.

Yet, also in these herbs, differences in vulnerability to water stress were observed on interspecific and intraspecific levels: in narrow-amplitude species, some key hydraulic parameters were correlated to the humidity conditions of their respective habitats (TLP, daily Ψ_{min}, P_{k50}, and P_{k88}), while other parameters ($k_{leaf\ max}$, $g_{s\ max}$, and P_{12CL}) did not reveal such trends. In contrast, the broad-amplitude species showed correlations or trends in intraspecific adjustment to different habitat conditions. Due to the ecological importance of herbaceous species in many ecosystems, better knowledge regarding their hydraulics will be essential to improve evaluations of water stress vulnerability on vegetation and ecosystem levels.

MATERIALS AND METHODS

Study Sites and Plant Material

The study was conducted at three sites in Innsbruck, Austria (47.267°N, 11.393°E), with 896.5 mm of precipitation and an average air temperature of 8.5°C in the 30-year mean (ZAMG Zentralanstalt für Meteorologie und Geodynamik, 2002). Three species of *Ranunculus*, which occur frequently within the study area, were chosen for analysis due to their differing habitat conditions. *Ranunculus bulbosus* is a typical species of dry meadows and nutrient-poor grasslands and grows up to 15 to 40 cm tall (Hegi, 1974; Fischer et al., 2008). This species dies back to perennial bulb-like corms in July and remains dormant until the following spring (Coles, 1973; Sarukhan, 1974). Sample plants were taken from a south-exposed, nonintensively managed meadow (Hötting). In contrast, *Ranunculus lanuginosus* is found in humid, shaded environments such as riparian forests or gorges and grows up to 50 to 70 cm (Hegi, 1974; Fischer et al., 2008). Plants were collected in a small gorge (Sillschlucht) at the south end of the city. The third species, *Ranunculus acris*, occurs in a range of humidity conditions from dry to humid meadows and reaches intermediate heights of 30 to 60 cm (Hegi, 1974; Polatschek, 2000; Fischer et al., 2008). For this species, a dry population cooccurring with the sampled *R. bulbosus* population and a humid population occurring on a separate high-humidity site (Völs) were used for analysis.

Soil humidity, species composition, and diurnal variation of g_s and Ψ_{leaf} were recorded on site in late spring and summer (May to August) in two consecutive years. For all other analyses, whole plants including major roots were collected from the field sites between May and August, immediately placed in dark plastic bags to limit water loss, and transported to the laboratory within 30 min. Plants were rehydrated overnight with their roots in water and covered with a dark plastic bag. Measurements were made on healthy, fully developed leaves including petioles (pressure-volume relations, leaf hydraulic vulnerability, and conductive xylem staining), leaf petioles with intact laminas (acoustic emissions), and leaf discs cut from the leaf laminas (electrolyte leakage).

Soil Humidity

Soil humidity was analyzed in situ in 2 years during dry periods with the Hydrosense II Soil Moisture Measurement System (Campbell Scientific), whereby volumetric SWC was measured 24 h after strong rainfall ($SWC_{field\ capacity}$) and after 7 d without rain (SWC_{dry}) in 10 samples per site and date. The SWC_{rel} (percentage of field capacity) after 7 d without rain was calculated as:

$$SWC_{rel} = \frac{SWC_{dry}}{mean\ (SWC_{field\ capacity})} \times 100 \quad (1)$$

Additionally, we recorded species composition at the three sites and characterized water availability using averaged ecological indicator values (humidity value; Ellenberg et al., 1992; Schaffers and Sykora, 2000).

Ψ Determination

Ψ_{leaf} was measured with a pressure chamber (Model 1000 Pressure Chamber; PMS Instrument) by applying pressure to an excised leaf sealed in the chamber, with the petiole protruding out through a rubber gasket (Scholander et al., 1965). Air pressure inside the chamber was increased slowly until the xylem sap meniscus became visible at the cutting site.

Pressure-Volume Analysis

Pressure-volume analyses (Tyree and Hammel, 1972; Sack and Pasquet-Kok, 2011; Bartlett et al., 2012) were carried out on five leaves per species/population to determine TLP, Π_0 at full turgor, and modulus of elasticity. Leaves were fully saturated before dehydration and regular measurements of Ψ_{leaf} and fresh weight. Relative water content was calculated from saturated, fresh, and dry weights and plotted against the inverse of Ψ_{leaf} to find the TLP (transition point between the linear and curved portions of the graph), Π_0 (negative inverse of the linear graph portion's intercept with the y axis), and modulus of elasticity (slope of the curve above and including the TLP). Parameters were calculated individually per leaf and then averaged per species/population.

Leaf Hydraulic Vulnerability

Declines in k_{leaf} due to increasing desiccation were analyzed with a modified non-steady-state leaf rehydration technique (Brodribb and Cochard, 2009; Blackman and Brodribb, 2011) and benchtop dehydration. For 39 to 45 leaves per species/population, we measured the decay of initial water uptake into the leaf from a small water container placed on a digital balance (CP64; Sartorius), which was connected to the leaf petiole via hydraulic tubing (see below).

At increasing levels of dehydration, plants were equilibrated in dark plastic bags and plant Ψ was determined on two leaves per plant. If Ψ between both leaves differed by 10% or less, the decay of initial flow was measured by excising a third leaf under water (including approximately 3 cm of the petiole), immediately connecting the leaf to hydraulic tubing, and covering the leaf with a moist paper towel to prevent transpiration. Thus, hydraulic flow was measured on non-light-acclimated, nontranspiring leaves. Flow rates (k_{leaf} [mmol m^{-2} s^{-1} MPa^{-1}]) were determined by linear regression of decreasing mass readings (water uptake) during the first 10 s and adjusted for

temperature and leaf area. $k_{leaf\ max}$ was calculated as the average of five maximum conductances observed per species/population. No cutting artifact (Wheeler et al., 2013) was expected for leaves excised under water (Scoffoni and Sack, 2015).

The reparameterized Weibull function (Ogle et al., 2009) was fitted to plots of relative k_{leaf} versus Ψ using the fitplc package for R version 3.1.1 (Duursma, 2014; R Core Team, 2014):

$$k = k_{leaf\ \ max}\left(1 - \frac{X}{100}\right)^{p}$$

$$p = \left[\left(\frac{P}{P_x}\right)^{\frac{P_x S_x}{V}}\right] \quad (2)$$

$$V = (X - 100)\ln\left(1 - \frac{X}{100}\right)$$

where k is the expected hydraulic conductance at X% loss of conductance, $k_{leaf\ max}$ is the k at full saturation (i.e. k at 0 MPa), P is the positive-valued Ψ ($P = -\Psi$), P_x is the Ψ at X% loss of conductance, and S_x is the slope of the vulnerability curve at $P = P_x$. P_{k50} and P_{k88} were defined as above.

Staining of Conducting Xylem Elements

To confirm the observed high levels of leaf hydraulic vulnerability, we stained conducting xylem elements in leaves of *R. acris* from the dry site. At increasing levels of dehydration, whole plants were equilibrated in dark plastic bags and plant Ψ was determined on one leaf per plant. Two additional leaves of the same plant were excised under water and immediately placed in a beaker containing (1) 1% (w/v) phloxine B (modified after Nardini et al., 2003) to reveal ongoing water transport in the lamina and (2) 0.05% (w/v) safranin (modified after Sperry et al., 1988b) to stain water-conducting conduits in the petioles. Samples were exposed to sunlight for about 10 min. Transpiration was favored by partially removing the cuticle and confirmed with an SC-1 Leaf Porometer (Decagon Devices). We analyzed images of the lamina taken with a digital camera and petiole cross sections (approximately 3 cm from the lamina) taken with a light microscope (Olympus BX41; Olympus Austria) and interfaced digital camera (ProgRes CT3; Jenoptik). To prevent artifacts by passive dye diffusion, only samples with unstained parenchyma and phloem were used.

Electrolyte Leakage

The vulnerability of living tissues to dehydration (Morin et al., 2007; Hu et al., 2010; Vilagrosa et al., 2010; Beikircher et al., 2013) was analyzed by benchtop dehydrating plants and comparing the leakage of electrolytes from 52 to 82 leaves per species at increasing levels of dehydration. After Ψ determination, three to 10 circular discs (0.6 cm in diameter) were cut from each leaf by use of a cork borer while avoiding major leaf veins. Leaf discs were pooled for each sample leaf, submerged in 15 mL of distilled water in individual centrifuge tubes, shaken for 24 h on a horizontal shaker (ST5 Bidimensional Shaker; CAT) at 5°C, followed by electrolytic conductivity measurement at room temperature (after 1 h of temperature equilibration) using a four-electrode conductivity sensor (Tetracon 325; WTW). Samples were then autoclaved at 120°C for 30 min and shaken overnight at room temperature, before final electrolytic conductivity was measured.

Relative electrolyte leakage (REL) was calculated as:

$$REL = \frac{C_1}{C_2} \times 100 \quad (3)$$

where C_1 and C_2 are the initial and final electrolytic conductivities, respectively. REL was then standardized to the percentage of cellular lysis by relating each sample's REL to the REL of the control (REL_c; Morin et al., 2007); in this case, samples were measured at Ψ of −0.2 MPa or greater:

$$Cellular\ lysis\ (\%) = \frac{REL - REL_c}{100 - REL_c} \times 100 \quad (4)$$

Vulnerability thresholds were again calculated by curve fitting to Equation 2, where k is the percentage of intact cells (k = 100 − the percentage of cellular lysis). The onset of damage to living cells (P_{12CL}) was defined as above.

Diurnal Variation of g_s and Ψ_{leaf}

We monitored the diurnal progression of g_s (using an SC-1 Leaf Porometer; Decagon Devices) and corresponding Ψ_{leaf} between sunrise and sunset on one clear, sunny day per species following a period of rainfall. For each data point, g_s was measured on the lower leaf side of four to five undamaged, fully developed leaves of different plants, whereas Ψ_{leaf} was determined on three undamaged, fully developed leaves of different plants.

Statistical Analyses

Data for curve fitting were pooled per species/population and method before further analysis. Vulnerability thresholds were statistically tested for differences using bootstrapped confidence intervals (n = 999 bootstrap estimates). Other data were normally distributed (QQ plots and Shapiro-Wilk test) and tested for differences using Student's t test (homoscedastic data as determined by the robust Brown-Forsythe Levene-type test) or Welch's two-sample t test (heteroscedastic data). All analyses were done in R version 3.1.1 (R Core Team, 2014) at a significance level of $P < 0.05$, whereas P was Bonferroni corrected for multiple comparisons. Values are presented as means ± SE or mean (lower confidence interval, upper confidence interval).

Supplemental Data

The following supplemental materials are available.

Supplemental Figure S1. Relative cumulative UE versus Ψ in *R. bulbosus*, *R. lanuginosus*, and dry and humid *R. acris* populations.

Supplemental Figure S2. Diurnal variation of Ψ and g_s in *R. bulbosus* and *R. lanuginosus*.

Supplemental Table S1. Species composition and ecological indicator values.

Supplemental Table S2. Water potential at 50 and 88% of total cumulative ultrasonic emissions above -3 MPa.

ACKNOWLEDGMENTS

We thank Dr. Georg Wohlfahrt for providing valuable microclimate data and Birgit Dämon for excellent technical assistance.

Received November 2, 2015; accepted February 5, 2016; published February 19, 2016.

LITERATURE CITED

Bartlett MK, Scoffoni C, Sack L (2012) The determinants of leaf turgor loss point and prediction of drought tolerance of species and biomes: a global meta-analysis. Ecol Lett **15:** 393–405

Beikircher B, De Cesare C, Mayr S (2013) Hydraulics of high-yield orchard trees: a case study of three *Malus domestica* cultivars. Tree Physiol **33:** 1296–1307

Beikircher B, Mayr S (2009) Intraspecific differences in drought tolerance and acclimation in hydraulics of *Ligustrum vulgare* and *Viburnum lantana*. Tree Physiol **29:** 765–775

Billings WD, Mooney HA (1968) Ecology of arctic and alpine plants. Biol Rev Camb Philos Soc **43:** 481–529

Blackman CJ, Brodribb TJ (2011) Two measures of leaf capacitance: insights into the water transport pathway and hydraulic conductance in leaves. Funct Plant Biol **38:** 118–126

Blackman CJ, Brodribb TJ, Jordan GJ (2010) Leaf hydraulic vulnerability is related to conduit dimensions and drought resistance across a diverse range of woody angiosperms. New Phytol **188:** 1113–1123

Blackman CJ, Brodribb TJ, Jordan GJ (2012) Leaf hydraulic vulnerability influences species' bioclimatic limits in a diverse group of woody angiosperms. Oecologia **168:** 1–10

Brodersen CR, McElrone AJ, Choat B, Lee EF, Shackel KA, Matthews MA (2013) In vivo visualizations of drought-induced embolism spread in *Vitis vinifera*. Plant Physiol **161:** 1820–1829

Brodribb TJ, Cochard H (2009) Hydraulic failure defines the recovery and point of death in water-stressed conifers. Plant Physiol **149:** 575–584

Brodribb TJ, Holbrook NM (2003) Stomatal closure during leaf dehydration, correlation with other leaf physiological traits. Plant Physiol **132:** 2166–2173

Brodribb TJ, Holbrook NM (2004) Stomatal protection against hydraulic failure: a comparison of coexisting ferns and angiosperms. New Phytol **162:** 663–670

Brodribb TJ, Holbrook NM (2005) Water stress deforms tracheids peripheral to the leaf vein of a tropical conifer. Plant Physiol **137:** 1139–1146

Bucci SJ, Scholz FG, Peschiutta ML, Arias NS, Meinzer FC, Goldstein G (2013) The stem xylem of Patagonian shrubs operates far from the point of catastrophic dysfunction and is additionally protected from drought-induced embolism by leaves and roots. Plant Cell Environ **36:** 2163–2174

Bunce JA (2006) How do leaf hydraulics limit stomatal conductance at high water vapour pressure deficits? Plant Cell Environ **29:** 1644–1650

Charra-Vaskou K, Charrier G, Wortemann R, Beikircher B, Cochard H, Ameglio T, Mayr S (2012) Drought and frost resistance of trees: a comparison of four species at different sites and altitudes. Ann For Sci **69:** 325–333

Chen JW, Zhang Q, Li XS, Cao KF (2009) Independence of stem and leaf hydraulic traits in six Euphorbiaceae tree species with contrasting leaf phenology. Planta **230:** 459–468

Choat B, Drayton WM, Brodersen C, Matthews MA, Shackel KA, Wada H, McElrone AJ (2010) Measurement of vulnerability to water stress-induced cavitation in grapevine: a comparison of four techniques applied to a long-vesseled species. Plant Cell Environ **33:** 1502–1512

Choat B, Jansen S, Brodribb TJ, Cochard H, Delzon S, Bhaskar R, Bucci SJ, Feild TS, Gleason SM, Hacke UG, et al (2012) Global convergence in the vulnerability of forests to drought. Nature **491:** 752–755

Cochard H (2002) A technique for measuring xylem hydraulic conductance under high negative pressures. Plant Cell Environ **25:** 815–819

Cochard H, Badel E, Herbette S, Delzon S, Choat B, Jansen S (2013) Methods for measuring plant vulnerability to cavitation: a critical review. J Exp Bot **64:** 4779–4791

Cochard H, Casella E, Mencuccini M (2007) Xylem vulnerability to cavitation varies among poplar and willow clones and correlates with yield. Tree Physiol **27:** 1761–1767

Cochard H, Delzon S, Badel E (2015) X-ray microtomography (micro-CT): a reference technology for high-resolution quantification of xylem embolism in trees. Plant Cell Environ **38:** 201–206

Coles S (1973) *Ranunculus bulbosus* L in Europe. Watsonia **9:** 207–228

Duursma R (2014) Fit vulnerability curves in R (R package). Bitbucket. https://bitbucket.org/remkoduursma/fitplc/ (January 10, 2015)

Ellenberg H, Weber EW, Wirth V, Werner W, Paulißen D (1992) Zeigerwerte von Pflanzen in Mitteleuropa. Scripta Geobotanica **18:** 1–258

Engelbrecht BMJ, Comita LS, Condit R, Kursar TA, Tyree MT, Turner BL, Hubbell SP (2007) Drought sensitivity shapes species distribution patterns in tropical forests. Nature **447:** 80–82

Fischer M, Oswald K, Adler W (2008) Exkursionsflora für Österreich, Liechtenstein und Südtirol, Ed 3. OÖ Landesmuseen, Land Öberösterreich, Linz, Austria

Frensch J, Hsiao TC (1994) Transient responses of cell turgor and growth of maize roots as affected by changes in water potential. Plant Physiol **104:** 247–254

Galmes J, Flexas J, Save R, Medrano H (2007) Water relations and stomatal characteristics of Mediterranean plants with different growth forms and leaf habits: responses to water stress and recovery. Plant Soil **290:** 139–155

Ganthaler A, Mayr S (2015) Dwarf shrub hydraulics: two *Vaccinium* species (*V. myrtillus, V. vitis-idaea*) of the European Alps compared. Physiol Plant **155:** 424–434

Gilliam FS (2007) The ecological significance of the herbaceous layer in temperate forest ecosystems. Bioscience **57:** 845–858

Gleason SM, Westoby M, Jansen S, Choat B, Hacke UG, Pratt RB, Bhaskar R, Brodribb TJ, Bucci SJ, Cao KF, et al (2016) Weak tradeoff between xylem safety and xylem-specific hydraulic efficiency across the world's woody plant species. New Phytol **209:** 123–136

Guyot G, Scoffoni C, Sack L (2012) Combined impacts of irradiance and dehydration on leaf hydraulic conductance: insights into vulnerability and stomatal control. Plant Cell Environ **35:** 857–871

Hao GY, Hoffmann WA, Scholz FG, Bucci SJ, Meinzer FC, Franco AC, Cao KF, Goldstein G (2008) Stem and leaf hydraulics of congeneric tree species from adjacent tropical savanna and forest ecosystems. Oecologia **155:** 405–415

Hao GY, Lucero ME, Sanderson SC, Zacharias EH, Holbrook NM (2013) Polyploidy enhances the occupation of heterogeneous environments through hydraulic related trade-offs in *Atriplex canescens* (Chenopodiaceae). New Phytol **197:** 970–978

Hegi G (1974) Illustrierte Flora von Mitteleuropa, Band III/3, Ed 2. Carl Hanser Verlag, Munich, Germany

Holloway-Phillips MM, Brodribb TJ (2011a) Minimum hydraulic safety leads to maximum water-use efficiency in a forage grass. Plant Cell Environ **34:** 302–313

Holloway-Phillips MM, Brodribb TJ (2011b) Contrasting hydraulic regulation in closely related forage grasses: implications for plant water use. Funct Plant Biol **38:** 594–605

Holste EK, Jerke MJ, Matzner SL (2006) Long-term acclimatization of hydraulic properties, xylem conduit size, wall strength and cavitation resistance in *Phaseolus vulgaris* in response to different environmental effects. Plant Cell Environ **29:** 836–843

Hu L, Wang Z, Du H, Huang B (2010) Differential accumulation of dehydrins in response to water stress for hybrid and common bermudagrass genotypes differing in drought tolerance. J Plant Physiol **167:** 103–109

Iovi K, Kolovou C, Kyparissis A (2009) An ecophysiological approach of hydraulic performance for nine Mediterranean species. Tree Physiol **29:** 889–900

Johnson DM, McCulloh KA, Woodruff DR, Meinzer FC (2012) Evidence for xylem embolism as a primary factor in dehydration-induced declines in leaf hydraulic conductance. Plant Cell Environ **35:** 760–769

Kikuta SB (2003) Ultrasound acoustic emissions from bark samples differing in anatomical characteristics. Phyton **43:** 161–178

Kim YX, Steudle E (2007) Light and turgor affect the water permeability (aquaporins) of parenchyma cells in the midrib of leaves of *Zea mays*. J Exp Bot **58:** 4119–4129

Kocacinar F, Sage RF (2003) Photosynthetic pathway alters xylem structure and hydraulic function in herbaceous plants. Plant Cell Environ **26:** 2015–2026

Kramer PJ, Boyer JS (1995) Water Relations of Plants and Soils. Academic Press, San Diego

Larcher W (1995) Physiological Plant Ecology. Ed 3. Springer, Berlin

Maherali H, Pockman WT, Jackson RB (2004) Adaptive variation in the vulnerability of woody plants to xylem cavitation. Ecology **85:** 2184–2199

Matzner SL, Rice KJ, Richards JH (2001) Intra-specific variation in xylem cavitation in interior live oak (*Quercus wislizenii* A. DC.). J Exp Bot **52:** 783–789

Mayr S, Rosner S (2011) Cavitation in dehydrating xylem of *Picea abies*: energy properties of ultrasonic emissions reflect tracheid dimensions. Tree Physiol **31:** 59–67

Mencuccini M (2003) The ecological significance of long-distance water transport: short-term regulation, long-term acclimation and the hydraulic costs of stature across plant life forms. Plant Cell Environ **26:** 163–182

Milburn JA, Johnson RPC (1966) The conduction of sap. II. Detection of vibrations produced by sap cavitation in Ricinus xylem. Planta **69:** 43–52

Monfreda C, Ramankutty N, Foley JA (2008) Farming the planet. 2. Geographic distribution of crop areas, yields, physiological types, and net primary production in the year 2000. Global Biogeochem Cycles **22:** Gb1022

Morin X, Améglio T, Ahas R, Kurz-Besson C, Lanta V, Lebourgeois F, Miglietta F, Chuine I (2007) Variation in cold hardiness and carbohydrate concentration from dormancy induction to bud burst among provenances of three European oak species. Tree Physiol **27:** 817–825

Nardini A, Pedà G, La Rocca N (2012) Trade-offs between leaf hydraulic capacity and drought vulnerability: morpho-anatomical bases, carbon costs and ecological consequences. New Phytol **196:** 788–798

Nardini A, Salleo S, Raimondo F (2003) Changes in leaf hydraulic conductance correlate with leaf vein embolism in *Cercis siliquastrum* L. Trees (Berl) **17:** 529–534

Nolf M, Creek D, Duursma R, Holtum J, Mayr S, Choat B (2015) Stem and leaf hydraulic properties are finely coordinated in three tropical rain forest tree species. Plant Cell Environ **38:** 2652–2661

Nolf M, Pagitz K, Mayr S (2014) Physiological acclimation to drought stress in *Solidago canadensis*. Physiol Plant **150:** 529–539

Ogle K, Barber JJ, Willson C, Thompson B (2009) Hierarchical statistical modeling of xylem vulnerability to cavitation. New Phytol **182:** 541–554

Polatschek A (2000) Flora von Nordtirol, Osttirol und Vorarlberg: Bd 3. Samenpflanzen: Fabaceae bis Rosaceae. Kartenteil. Tiroler Landesmuseum Ferdinandeum, Innsbruck, Austria

Ponomarenko A, Vincent O, Pietriga A, Cochard H, Badel É, Marmottant P (2014) Ultrasonic emissions reveal individual cavitation bubbles in water-stressed wood. J R Soc Interface **11:** 20140480

R Core Team (2014) R: A Language and Environment for Statistical Computing. http://www.R-project.org/

Rejmanek M (1999) Invasive plant species and invasible ecosystems. *In* OT Sandlund, PJ Schei, A Viken, eds, Invasive Species and Biodiversity Management. Kluwer Academic Publishers, Dordrecht, The Netherlands, pp 79–102

Rosenthal DM, Stiller V, Sperry JS, Donovan LA (2010) Contrasting drought tolerance strategies in two desert annuals of hybrid origin. J Exp Bot **61:** 2769–2778

Rosner S (2015) A new type of vulnerability curve: is there truth in vine? Tree Physiol **35:** 410–414

Sack L, Holbrook NM (2006) Leaf hydraulics. Annu Rev Plant Biol **57:** 361–381

Sack L, Pasquet-Kok J (2011) Leaf pressure-volume curve parameters. PrometheusWiki. http://www.publish.csiro.au/prometheuswiki/tiki-pagehistory.php?page=Leaf%20pressure-volume%20curve%20parameters&preview=16 (January 22, 2015)

Sandford AP, Grace J (1985) The measurement and interpretation of ultrasound from woody stems. J Exp Bot **36:** 298–311

Sarukhan J (1974) Studies on plant demography: *Ranunculus repens* L., *R. bulbosus* L. and *R. acris* L. II. Reproductive strategies and seed population dynamics. J Ecol **62:** 151–177

Schaffers AP, Sykora KV (2000) Reliability of Ellenberg indicator values for moisture, nitrogen and soil reaction: a comparison with field measurements. J Veg Sci **11:** 225–244

Scholander PF, Bradstreet ED, Hemmingsen EA, Hammel HT (1965) Sap pressure in vascular plants: negative hydrostatic pressure can be measured in plants. Science **148:** 339–346

Scholz FG, Bucci SJ, Hoffmann WA, Meinzer FC, Goldstein G (2010) Hydraulic lift in a neotropical savanna: experimental manipulation and model simulations. Agric For Meteorol **150:** 629–639

Scoffoni C, Sack L (2015) Are leaves 'freewheelin'? Testing for a Wheeler-type effect in leaf xylem hydraulic decline. Plant Cell Environ **38:** 534–543

Scoffoni C, Vuong C, Diep S, Cochard H, Sack L (2014) Leaf shrinkage with dehydration: coordination with hydraulic vulnerability and drought tolerance. Plant Physiol **164:** 1772–1788

Sperry JS, Donnelly JR, Tyree MT (1988a) A method for measuring hydraulic conductivity and embolism in xylem. Plant Cell Environ **11:** 35–40

Sperry JS, Donnelly JR, Tyree MT (1988b) Seasonal occurrence of xylem embolism in sugar maple (*Acer saccharum*). Am J Bot **75:** 1212–1218

Sperry JS, Holbrook NM, Zimmermann MH, Tyree MT (1987) Spring filling of xylem vessels in wild grapevine. Plant Physiol **83:** 414–417

Stiller V, Lafitte HR, Sperry JS (2003) Hydraulic properties of rice and the response of gas exchange to water stress. Plant Physiol **132:** 1698–1706

Stiller V, Sperry JS (2002) Cavitation fatigue and its reversal in sunflower (*Helianthus annuus* L.). J Exp Bot **53:** 1155–1161

Tixier A, Cochard H, Badel E, Dusotoit-Coucaud A, Jansen S, Herbette S (2013) *Arabidopsis thaliana* as a model species for xylem hydraulics: does size matter? J Exp Bot **64:** 2295–2305

Tyree MT, Davis SD, Cochard H (1994) Biophysical perspectives of xylem evolution: is there a tradeoff of hydraulic efficiency for vulnerability to dysfunction. IAWA J **15:** 335–360

Tyree MT, Ewers FW (1991) The hydraulic architecture of trees and other woody plants. New Phytol **119:** 345–360

Tyree MT, Fiscus EL, Wullschleger SD, Dixon MA (1986) Detection of xylem cavitation in corn under field conditions. Plant Physiol **82:** 597–599

Tyree MT, Hammel HT (1972) Measurement of turgor pressure and water relations of plants by pressure-bomb technique. J Exp Bot **23:** 267–282

Tyree MT, Sperry JS (1989) Vulnerability of xylem to cavitation and embolism. Annu Rev Plant Physiol **40:** 19–38

Tyree MT, Zimmermann MH (2002) Xylem Structure and the Ascent of Sap, Ed 2. Springer, Berlin

Vilagrosa A, Morales F, Abadia A, Bellot J, Cochard H, Gil-Pelegrin E (2010) Are symplast tolerance to intense drought conditions and xylem vulnerability to cavitation coordinated? An integrated analysis of photosynthetic, hydraulic and leaf level processes in two Mediterranean drought-resistant species. Environ Exp Bot **69:** 233–242

Wagner KR, Ewers FW, Davis SD (1998) Tradeoffs between hydraulic efficiency and mechanical strength in the stems of four co-occurring species of chaparral shrubs. Oecologia **117:** 53–62

Wheeler JK, Huggett BA, Tofte AN, Rockwell FE, Holbrook NM (2013) Cutting xylem under tension or supersaturated with gas can generate PLC and the appearance of rapid recovery from embolism. Plant Cell Environ **36:** 1938–1949

Wohlfahrt G, Irschick C, Thalinger B, Hörtnagl L, Obojes N, Hammerle A (2010) Insights from independent evapotranspiration estimates for closing the energy balance: a grassland case study. Vadose Zone J **9:** 1025–1033

Wolkerstorfer SV, Rosner S, Hietz P (2012) An improved method and data analysis for ultrasound acoustic emissions and xylem vulnerability in conifer wood. Physiol Plant **146:** 184–191

ZAMG Zentralanstalt für Meteorologie und Geodynamik (2002) Klimadaten von Österreich 1971-2000. http://www.zamg.ac.at/fix/klima/oe71-00/klima2000/klimadaten_oesterreich_1971 _ frame1.htm (January 22, 2015)